
Clinical Evaluation of ^{99m}Tc -Rituximab for Sentinel Lymph Node Mapping in Breast Cancer Patients

Nan Li*¹, Xuejuan Wang*¹, Baohe Lin¹, Hua Zhu¹, Cheng Liu¹, Xiaobao Xu¹, Yan Zhang¹, Shizhen Zhai¹, Tao OuYang², Jinfeng Li², and Zhi Yang¹

¹Key Laboratory of Carcinogenesis and Translational Research (Ministry of Education), Department of Nuclear Medicine, Peking University Cancer Hospital & Institute, Beijing, China; and ²Breast Center, Peking University Cancer Hospital & Institute, Beijing, China

The metastatic status of sentinel lymph nodes (SLNs) might be the most important prognostic factor in breast cancer. In this paper, we report to our knowledge the first study of ^{99m}Tc -rituximab as a radiotracer for imaging of SLNs using lymphoscintigraphy in both preoperative and intraoperative breast cancer patients. **Methods:** ^{99m}Tc -rituximab was designed as an SLN tracer targeting the CD20 antigen, which expresses extensively in LNs. A retrospective study was performed on 2,317 patients with primary breast cancer who underwent lymphoscintigraphy and sentinel lymph node biopsy (SLNB). Before imaging, all patients were administered a preoperative peritumoral injection of 37 MBq of ^{99m}Tc -rituximab. **Results:** ^{99m}Tc -rituximab was synthesized in both high radiolabeling yield and high radiochemical purity (>95%), with molecular integrity and immune activity well maintained. The initial study of 100 breast cancer patients showed that the success rate of SLN lymphoscintigraphy by injection of ^{99m}Tc -rituximab, as compared with SLNB, was 100%, and the sensitivity, specificity, accuracy, and false negative rate were 97.4%, 100%, 98.0%, and 2.60%, respectively. Of the following 2,217 patients studied, the success rate of lymphoscintigraphy and SLNB was 98.8% and 99.9%, and the average number of SLN was 1.78 (range, 1–10) and 2.85 (range, 1–15). Age was an independent predictor of the number of SLNs identified by lymphoscintigraphy and intraoperative handheld γ -probe ($P < 0.05$), and other factors—such as sex, imaging time, primary tumor site, histopathologic subtype, clinical T stage, and immunochemistry—were not ($P > 0.05$). However, the SLN metastatic rates were different in patients with different histopathologic subtype, clinical T stage, and immunochemistry ($P < 0.05$). **Conclusion:** Here we report the first study of the new radiotracer ^{99m}Tc -rituximab for breast cancer lymphoscintigraphy. This tracer showed great feasibility, safety, and effectiveness for SLN mapping in breast cancer patients.

Key Words: ^{99m}Tc -rituximab; sentinel lymph node mapping; breast cancer; lymphoscintigraphy

J Nucl Med 2016; 57:1214–1220

DOI: 10.2967/jnumed.115.160572

Accurate lymph node (LN) staging is essential for the prognosis and treatment of cancer patients. The term sentinel lymph node (SLN) is defined as the first node or nodes in the lymphatic drainage of the primary tumor and was so named by Gould et al. in 1960 (1). In 1977, Cabanas suggested that the SLN would be predictive of metastatic spread to the respective regional lymphatic basins (2). SLN mapping also enables surgeons to perform a minimally invasive biopsy of the SLN and to completely resect all SLNs, and in the past 2 decades, the detection and biopsy of SLNs have already been implemented in the surgical treatment of breast cancer and malignant melanoma patients (3,4).

Visual examination with blue dyes and lymphoscintigraphy has been extensively used for SLN mapping in the clinic (5). Isosulfan blue and methylene blue are 2 commonly used blue dyes in the SLN biopsy of breast cancer. Actually, methylene blue is the most commonly used SLN mapping agent in China. However, the small-molecule blue dyes migrate rapidly in the lymphatics, and the retention of dye in SLNs is poor (<5 min) (6). So, it is essential for surgeons to locate and remove the SLNs quickly before the dye spreads to other nodes. Moreover, the blue dyes may also cause unwanted anaphylactic side effects and cause blue discoloration of urine, stool, and skin in some patients (7). For lymphoscintigraphy, a variety of radiopharmaceuticals has been used including the filtered and unfiltered ^{99m}Tc -sulfur colloid, ^{99m}Tc -labeled albumin-based colloids, and ^{99m}Tc -antimony trisulfide colloid. For all these colloid-based imaging techniques, SLN visualization depends on the transport of the radiolabeled particles from the injection site to SLNs through lymphatic channels (8). The radiolabeled particles are then trapped in the node and absorbed by macrophages. The detection rate of these ^{99m}Tc radiopharmaceuticals (range, 86%–99%) (9,10) is mainly caused by many factors, such as particle size, particle concentration, and injection dose, that can influence the transport and accumulation process of the tracer (11–13).

In 2013, The U.S. Food and Drug Administration approved Lymphoseek (^{99m}Tc -tilmanocept; Navidea Biopharmaceuticals, Inc.) as the radiotracer for detecting SLN in breast cancer and melanoma patients (14,15). The success of Lymphoseek encourages us to report other receptor-targeted SLN imaging agents. Rituximab is a chimeric monoclonal antibody against the CD20 antigen presenting on the membrane of pre-B and mature B lymphocytes. It was approved by the Food and Drug Administration in 1997 to treat B cell non-Hodgkin lymphomas resistant to chemotherapy regimens (16,17). Considering there are a large number of

Received May 14, 2015; revision accepted Feb. 18, 2016.
For correspondence or reprints contact either of the following:
Nan Li, Department of Nuclear Medicine, Beijing Cancer Hospital, No. 52 Fucheng Rd., Beijing, 100142, China.
E-mail: rainbow6238@sina.com
Zhi Yang, Department of Nuclear Medicine, Beijing Cancer Hospital, No. 52 Fucheng Rd., Beijing, 100142, China.
E-mail: pekyz@163.com
*Contributed equally to this work.
Published online Mar. 16, 2016.
COPYRIGHT © 2016 by the Society of Nuclear Medicine and Molecular Imaging, Inc.

TABLE 1
Quality Control of ^{99m}Tc-Rituximab for Clinical Application

Parameter	QC specification	QC result
Appearance	Clear, colorless	Pass
Volume	0.5–1.0 mL	0.5 mL
Injection dose	18.5–37 MBq	37 MBq
pH	4.0–8.0	7.0
Radio–thin-layer chromatography	>95%	>99%
Radio–high-performance liquid chromatography	>95%	>99%
Ethanol	<5%	0
Endotoxins	<15 EU/mL	Pass
Sterility	Sterile	Pass
Specific activity	111 GBq/μmol	Pass

B cells presenting in LNs, we hypothesized that radiolabeled rituximab can serve as an effective imaging tool for SLN identification. Therefore, in this work rituximab was directly labeled with the most widely used SPECT radionuclide, ^{99m}Tc. The resultant tracer, ^{99m}Tc-rituximab, was further evaluated in a large cohort of breast cancer patients (total no. of patients = 2,317). Here the feasibility, effectiveness, and safety of using ^{99m}Tc-rituximab for clinical imaging of SLN were reported.

MATERIALS AND METHODS

Patients

The criterion for inclusion and exclusion of patients meets standard SLN biopsy criteria (supplemental materials [available at <http://jnm.snmjournals.org>]). The clinical trial was approved by Peking University Cancer Hospital & Institute. From July 2005 to June 2011, patients with breast cancer were recruited at Peking University Cancer Hospital & Institute. The patients' informed consent was obtained before the tests. SLN imaging was performed in 2,317 breast cancer patients using ^{99m}Tc-rituximab followed by SLN biopsy to verify the imaging results.

Radiotracer Preparation

^{99m}Tc radiolabeling of rituximab and radio–high-performance liquid chromatography analysis was performed as described (Supplemental Figs. 1–3). Briefly, rituximab (10 mg, 70 nmol) was dissolved in 1 mL of phosphate-buffered solution (pH 7.4, 10 mM), and 0.3 mL of the solution were taken out to react with 25 μL of 10% (V/V) 2-mercaptoethanol for 15 min in the dark. The product was then purified by a PD-10 column to obtain 2 mL of reduced rituximab, the solution was divided into 0.2 mL for each vial, and the samples were stored at –20°C for further use. When radiolabeling was performed, 0.2 mL of solution of reduced rituximab was warmed to room temperature and added to 10 μL of glucoheptonic acid (100 mg/mL), 15 μL of SnCl₂ (1 mg/mL), and 370–470 MBq of Na^{99m}TcO₄. The reaction mixture was shaken at room temperature for 10 min. ^{99m}Tc-rituximab was then purified by a PD-10 column. For clinical use, the radiochemical purity of the tracer was always > 99% tested by radio–thin-layer chromatography and radio–high-performance liquid chromatography. The radiotracer solution was then diluted to approximately 74 MBq/mL (2 mCi/mL) with saline and was filtered with a 0.20-μm Millex-LG filter (EMD Millipore). The synthesis of Rit-SH and radiolabeling with ^{99m}Tc were performed under good-manufacturing-practice conditions

with daily quality control. Each patient was injected with 37 MBq (1.0 mCi) of ^{99m}Tc-rituximab.

Lymphatic Mapping Protocol

Guided by ultrasound, all patients were administered peritumoral subcutaneous injections of ^{99m}Tc-rituximab (37.0 MBq, 0.5 mL) 2–18 h before biopsy. In lymphoscintigraphy, 3 point sources (0.37 MBq) were put on the surface of the patient to mark the sternal notch, contralateral sternal margin, and metasternum location as references. Planar lymphoscintigraphy was then acquired by a SPECT system (Siemens; E.Cam) with the patient positioned supine in the anterior view and the ipsilateral lateral view, to determine the location and number of SLNs (Supplemental Figs. 4–8). Acquisition parameters

TABLE 2
Clinical Pathologic Characteristics of 100 Breast Cancer Patients

Characteristic	No. of patients
Sex	
Female	100
Age (y)	
≤50	49
>50	51
Left or right side breast cancer	
Left	45
Right	55
Imaging time after injection of tracer	
2–4 h	28
16–18 h	72
Primary tumor location	
Upper inner quadrant	26
Lower inner quadrant	7
Upper outer quadrant	49
Lower outer quadrant	16
Central portion	2
Histopathologic type	
Invasive ductal carcinoma	88
Invasive lobular carcinoma	4
Other	8
Clinical T stage	
Tis	1
T1	25
T2	65
T3	9
ER/PR/HER2	
+/+/+	23
-/-/+	11
+/-/- or -/+/- or +/-/-	49
+/-/+ or -/+/+	11
-/-/-	6

ER = estrogen receptor; PR = progesterone receptor; HER2 = human epidermal growth factor receptor-2.

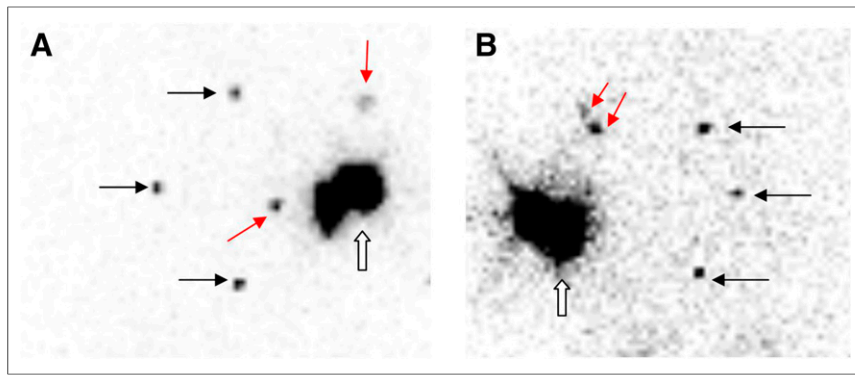


FIGURE 1. SLN imaging of breast cancer patients after injection of ^{99m}Tc -rituximab (black arrow, point source on patient body surface to mark sternal notch, contralateral sternal margin, and metasternum; red arrow, SLNs; hollow arrow, injection site). (A) One SLN in axilla and 1 SLN in intramammary. (B) Two SLNs in axilla.

were as follows: low-energy high-resolution parallel-hole collimator; energy peak, 140 keV; 20% window width; 128×128 matrix; and zoom, 1.

Surgical Procedure

After axillary incision, SLNs were identified by a handheld γ -detecting probe (Crystal). All radioactive nodes with a counting rate of 10% or greater of the hottest node were removed. During surgery, all the SLNs were evaluated by frozen-section analysis. During the initial learning period (100 patients), all the patients underwent an axillary LN dissection (ALND). After initial learning, only patients with positive frozen sections immediately underwent an ALND. To evaluate the effectiveness and reliability of ^{99m}Tc -rituximab, another 2,217 patients were divided into different groups to find the predictors of the number of SLNs identified. All the dissected SLNs and non-SLNs were analyzed by hematoxylin and eosin staining.

Statistical Analysis

All values are expressed as mean \pm SD. Statistical analysis was performed using the 1-way ANOVA or the χ^2 test by SPSS17.0 (SPSS Inc.). The differences between groups were considered to be significant when the *P* values were < 0.05 .

RESULTS

Synthesis of ^{99m}Tc -Rituximab

The radiolabeling yield was $> 95\%$ using the freeze-dried kit of rituximab and $\text{Na}^{99m}\text{TcO}_4$. Radio-thin-layer chromatography analysis was used, and *R_f* values were 0–0.1 and 0.9–1 for ^{99m}Tc -rituximab and $\text{Na}^{99m}\text{TcO}_4$, respectively (Supplemental Fig. 2). The radiochemical purity of ^{99m}Tc -rituximab was $> 99\%$, with the retention time (*t_R*) of 6.69 min by radio-high-performance liquid chromatography (Supplemental Fig. 3). ^{99m}Tc -rituximab was prepared and checked for quality control before clinical patient imaging (Table 1).

Clinical Application of ^{99m}Tc -Rituximab in Initial Learning Period

Of the randomly assigned 100 patients, the median age was 46 y (range, 27–73 y), and the median tumor size was 2.15 cm (range, 0.60–7.20 cm). Other clinical pathologic features of this patient group are shown in Table 2.

Lymphoscintigraphy or lymphatic mapping was acquired 2–4 h after injection in 28 patients and 16–18 h after injection in 72

cases. The typical cases of lymphoscintigraphy are shown in Figure 1.

Sentinel Lymph Node Biopsy (SLNB)

SLNs were identified in all 100 patients; the detection rate was 100% (100/100). One hundred seventy SLNs were identified, 163 in the axilla and 7 in the internal mammary nodes (average, 1.7 [range, 1–5 SLNs] per patient). Lymphoscintigraphy also revealed SLNs ≥ 3 in 18 patients and SLNs < 3 in 72 patients. SLNs were found in both axilla and internal mammary nodes for 4 patients, only in internal mammary nodes for 1 patient, and only in axilla for 95 patients.

SLNs were harvested in 100 patients as guided by a handheld γ -detecting probe, and the success rate of SLNB was 100%

(100/100). In total, 262 SLNs were harvested through SLNB, an average of 2.62 (range, 1–7) SLNs per patient. γ -probe detection revealed SLNs ≥ 3 in 42 patients and SLNs < 3 in 58 patients. Interestingly the number of SLNs identified by intraoperative detection was higher than that of SLN imaging in 49 patients and was equal in 51 patients. One hundred nine of 262 SLNs (41.6%) were confirmed metastases, and 75 of 100 patients (75%) were classified as metastatic by pathologic examination (average, 1.45 [range, 1–5] metastatic SLNs per patient).

In this initial study, 1,504 LNs were removed in ALND (average, 15.04 [range, 1–39] LNs per patients). And the metastatic rate was 5.85% (88/1,504 LNs). On the basis of patients, the pathologic diagnosis of SLNs and LNs in ALND are shown in Table 3. The sensitivity, specificity, and accuracy of SLNB was 97.40% (75/77), 100% (23/23), and 98% (98/100), respectively. And the false-negative rate of SLNB was 2.60% (2/77).

Lymphoscintigraphy and SLNB of 2,217 Breast Cancer Patients

Retrospective studies of another 2,217 patients with primary breast cancer were conducted. The median patient age was 51 y (range, 21–92 y), and the median tumor size was 1.94 cm (range, 0.4–11.9 cm). When 4 patients with bilateral breast cancer were also considered, lymphoscintigraphy was performed in 2,221 cases, of which 923 were acquired at 2–4 h after injection and 1,298 at 16–18 h after injection. No LN was shown in 27 cases (Table 4). Therefore the success rate of this imaging study was 98.78% (2,194/2,221).

TABLE 3
Pathologic Comparison Between SLNs and LNs in ALND

Group	Metastatic SLN	Nonmetastatic SLN	Total
Metastatic LNs in ALND	26	2	28
Nonmetastatic LNs in ALND	49	23	72
Total	75	25	100

In total, 3,896 SLNs were found, 3,576 SLNs in the axilla, 290 in the internal mammary nodes, and 30 in the infraclavicular, with an average of 1.78 (range, 1–10) SLNs per case. Moreover, it was found that there were 3 or more SLNs in 394 cases and fewer than 3 SLNs in 1,800 cases. SLNs were found in 182 cases in both axilla and internal mammary nodes, 25 cases in both axilla and supraclavicular nodes, 19 cases in both axilla and intramammary, 10 cases only in internal mammary nodes, and 1,958 cases only in axilla. The frequency of extraaxillary SLNs was 10.76%, and the frequency of drainage to internal mammary nodes was 8.34%.

TABLE 4
Analysis of 27 Patients in Whom Lymphoscintigraphy Failed to Identify LNs

Characteristic	Patient	Percentage
Sex		
Female	27	100%
Age		
≤50	10	37.04%
>50	17	62.96%
Left or right cancer		
Left	17	62.96%
Right	10	37.04%
Imaging time		
2–4 h after injection	13	48.15%
16–18 h after injection	14	51.85%
Primary tumor site		
Upper inner quadrant	26	96.30%
Lower inner quadrant	7	25.93%
Upper outer quadrant	49	181.48%
Lower outer quadrant	16	59.26%
Central portion	2	7.41%
Histopathologic type		
Ductal	24	88.89%
Lobular	1	3.70%
Other	2	7.41%
Clinical T stage		
T1	10	37.04%
T2	16	59.26%
T3	1	3.70%
ER/PR/HER2		
+/+/+	5	18.52%
-/-/+	4	14.81%
+/-/- or -/+/- or +/-/-	14	51.85%
+/-/+ or -/+/+	3	11.11%
-/-/-	1	3.70%
Pathology of SLN		
Metastatic SLN	19	70.37%
Nonmetastatic SLN	8	29.63%

ER = estrogen receptor; PR = progesterone receptor; HER2 = human epidermal growth factor receptor-2.

SLNs were harvested in 2,218 cases (SLNs ≥ 3 in 1,064 cases, and SLNs < 3 in 1,154 cases) by a handheld γ -detecting probe, and the success rate of SLNB was 99.86% (2,218/2,221). In total, 6,313 SLNs were harvested in SLNB (average, 2.85 [range, 1–15] SLNs per case). The number of SLNs in intraoperative detection was more than SLN imaging in 1,432 cases and was equal in 786 cases. Eight hundred three of 6,313 (12.72%) SLNs and 560 of 2,218 cases (25.25%) were confirmed metastases by pathology (average, 1.43 [range, 1–10] metastatic SLNs per case). The results of lymphoscintigraphy and SLNB of these 2,217 breast cancer patients are summarized in Table 5 and Figure 2.

We also found that age was an independent predictor. On average, patients younger than 50 y have more SLNs identified than those older than 50 y whether detected by lymphoscintigraphy (average, 1.85 vs. 1.65, $P < 0.001$) or by intraoperative handheld γ -probe (average, 2.96 vs. 2.72, $P = 0.002$). And sex, imaging time, primary tumor site, histopathologic subtype, clinical T stage, and immunochemistry were not independent predictors of the number of SLNs ($P > 0.05$). However, the SLN metastatic rates were different in patients with different histopathologic subtype, clinical T stage, and immunochemistry ($P < 0.05$) and had no relationship with sex, imaging time, and primary tumor sites ($P > 0.05$).

DISCUSSION

SLNB is a validated technique that enables acute LN staging with low morbidity. It has been widely used as the preferred alternative to ALND in breast cancer patients. Many ^{99m}Tc radiopharmaceuticals used in the clinic, such as ^{99m}Tc -sulfur colloid, are all colloids that reveal SLN by phagocytosis of reticuloendothelial cells in LNs (18). However, the detection rate of lymphoscintigraphy and SLNB using these tracers is directly influenced by the size of particles prepared and can thus show large variation (19,20). The radiotracer developed in this study is a novel SPECT probe of SLN detection, which contains ^{99m}Tc -labeled monoclonal antibody–targeting CD20 abundantly expressed on the surface of B cells in LNs. Compared with the colloidal radiotracer, the advantage of ^{99m}Tc -rituximab is its uniform molecular weight and molecular size. So if the technical factors (such as the injection dose, injection volume, and injection site) are well controlled, as we have done in this study, ^{99m}Tc -rituximab will not escape easily from SLNs to the second-echelon LNs. Therefore, the clear SLN imaging in patients and the high success rate of lymphoscintigraphy and SLNB in our study is not a great surprise.

2-mercapitoethanol is a common antibody reduction agent that can well retain the molecular integrity and immune activity of antibody (21). After modification by 2-mercapitoethanol, rituximab is easy to radiolabel with ^{99m}Tc , with high labeling yield and radiochemical purification (>95%). Although the uptake of SLN in rats reaches the maximum at 4 h after subcutaneous injection, the high SLN-to-injection site ratio can remain to even 18 h after injection (22). (These data are not presented in this paper.) The high SLN-to-injection site ratio made it possible for the patients to be administered the radiotracer either the day before or on the same day as SLNB operation.

SLNB is a combined effort involving at least 3 different specialties: nuclear medicine, surgical oncology, and pathology. The learning curve reflects the understanding and proficiency among different operators. Previous studies have shown the importance of learning curve (23–25). For example, the National

TABLE 5
Lymphoscintigraphy and SLNB of 2,217 Breast Cancer Patients

Characteristic	No. of patients	Lymphoscintigraphy		Intraoperative SLN detection		SLN pathology	
		SLNs ($\bar{x} \pm s$)	Significance	SLNs ($\bar{x} \pm s$)	Significance	Patients with metastatic SLNs	Significance
Total	2,217	1.76 ± 1.08		2.85 ± 1.86			
Sex			<i>P</i> = 0.377		<i>P</i> = 0.613		<i>P</i> = 0.411
Female	2,215	1.76 ± 1.08		2.50 ± 0.71		560	
Male	2	2.50 ± 0.71		2.85 ± 1.87		0	
Age			<i>P</i> = 0.000		<i>P</i> = 0.002		<i>P</i> = 0.355
≤50	1,182	1.85 ± 1.13		2.96 ± 1.89		308	
50	1,035	1.65 ± 1.00		2.72 ± 1.83		252	
Left or right cancer			<i>P</i> = 0.651		<i>P</i> = 0.719		<i>P</i> = 0.371
Bilateral	4	2 ± 0.82		3.00 ± 1.16		2	
Left	1,140	1.74 ± 1.02		2.82 ± 1.84		279	
Right	1,073	1.78 ± 1.13		2.88 ± 1.89		279	
Imaging time			<i>P</i> = 0.275		<i>P</i> = 0.897		<i>P</i> = 0.834
2–4 h after injection	922	1.73 ± 1.04		2.85 ± 1.80		235	
16–18 h after injection	1,295	1.78 ± 1.10		2.84 ± 1.91		325	
Primary tumor site			<i>P</i> = 0.080		<i>P</i> = 0.316		<i>P</i> = 0.166
Upper inner quadrant	302	1.85 ± 0.98		2.66 ± 1.70		66	
Lower inner quadrant	254	1.67 ± 0.89		2.83 ± 1.90		54	
Upper outer quadrant	882	1.79 ± 1.19		2.89 ± 1.94		243	
Lower outer quadrant	438	1.75 ± 1.13		2.94 ± 1.76		110	
Central portion	341	1.65 ± 0.89		2.81 ± 1.90		87	
Histopathologic subtype			<i>P</i> = 0.178		<i>P</i> = 0.398		<i>P</i> = 0.000
Ductal	1,821	1.74 ± 1.06		2.83 ± 1.84		484	
Lobular	179	1.90 ± 1.22		2.85 ± 1.85		49	
Other	217	1.76 ± 1.09		3.01 ± 2.07		27	
Clinical T stage			<i>P</i> = 0.098		<i>P</i> = 0.191		<i>P</i> = 0.002
Tis	58	1.90 ± 1.07		3.10 ± 2.26		4	
T1	1,179	1.73 ± 1.05		2.79 ± 1.84		294	
T2	907	1.77 ± 1.09		2.88 ± 1.85		249	
T3	73	2.01 ± 1.23		3.16 ± 2.10		13	
ER/PR/HER2			<i>P</i> = 0.311		<i>P</i> = 0.973		<i>P</i> = 0.000
+ / + / +	634	1.78 ± 1.12		2.81 ± 1.86		187	
- / - / +	329	1.83 ± 1.04		2.87 ± 1.56		68	
+ / - / - or - / + / - or + / + / -	902	1.70 ± 1.04		2.85 ± 1.95		243	
+ / - / + or - / + / +	150	1.86 ± 1.09		2.86 ± 1.89		31	
- / - / -	202	1.79 ± 1.22		2.92 ± 1.93		31	

Surgical Adjuvant Breast and Bowel Project (NSABP) trial B-32 proved that the success rate of SLN biopsy was affected by the learning curve.

In our study, 100 patients were studied to learn the accuracy and false-negative rate of SLNB compared with ALND in the learning period. The success rate of SLNB was 100%, and the false-negative rate was 2.60%, which is better than that of other studies (false-negative rate ranging from 6% to 10%) (26,27).

Although a combination of blue dye and radiotracer has been described previously to be a superior method of detecting SLNs in breast cancer patients, with an identification rate of 89%–97%, the ^{99m}Tc radioisotopes can be used alone, with an identification rate of 86%–99% (9,10). In this study, ^{99m}Tc-rituximab alone was chosen as an SLN agent without being combined with blue dye, and the technical factors including the injection dose, injection volume, and injection site were well controlled to reduce interference. The

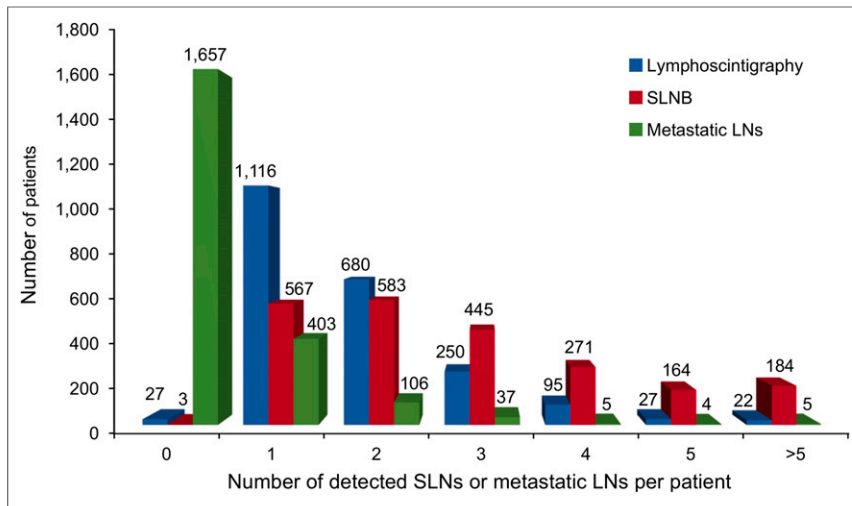


FIGURE 2. Lymphoscintigraphy and SLNB frequency distribution results in these 2,217 breast cancer patients.

retrospective analyses of 2,217 patients show that the identification rates of lymphoscintigraphy and intraoperation handheld γ -probe were 98.78% and 99.86%, respectively. The detailed analyses found that lymphoscintigraphy failed to identify LNs in 27 patients, and most were patients older than 50 y or with metastatic SLNs, as shown in Table 4.

The number of SLNs in our study (average, 2.85; range, 1–15) is consistent with results of other investigators (average, 2 [range, 1–18]; and average, 2.8 [range, 1–15]) (28,29). As to the location of SLNs in these studies, lymphatic drainage from the breast was described to include the axilla, internal mammary chain, supraclavicular nodes, interpectoral nodes, and intramammary LNs (30,31), which were clearly displayed using lymphoscintigraphy. The SLNs in previous studies were found in the axilla, internal mammary, and supraclavicular nodes. But the frequency of extraaxillary SLNs including internal mammary nodes was slightly lower than in previous studies (10.76% vs. 17%–56% and 8.34% vs. 10%–40%, respectively) (32–35).

Because of our strict quality control and the high specific activity of ^{99m}Tc -rituximab (111 GBq/ μmol) used, no side effect was observed in the study of 2,317 patients. The injection dose for each patient was 37 MBq, and this corresponded to about 50 μg of rituximab, which is less than the amount of rituximab used for skin testing for allergies (36). The radioactivity dose used here was much lower than that of ^{99m}Tc -MDP (370–740 MBq) used for bone scanning. Our study indicates that ^{99m}Tc -rituximab can be used safely for patient imaging. In addition, ^{99m}Tc -rituximab could also be used for lymphoscintigraphy in melanoma, for which more frequent aberrant drainage is anticipated, and SLNB imaging is more challenging. The ^{99m}Tc -rituximab radiotracer showed promising results in lymphoscintigraphy of melanoma. Further clinical research and related evaluation on melanoma lymphoscintigraphy will be reported in due course.

CONCLUSION

^{99m}Tc -rituximab is a novel lymph imaging agent that can specifically bind with the protein CD20 expressed on the surface of B cells in LNs. The labeling method is simple, with a high radiolabeling yield and intact immune activity. Lymphoscintigraphy in

breast cancer patients has shown good SLN identification. And its feasibility, safety, and effectiveness have been confirmed by clinical SLNB application with large samples.

DISCLOSURE

The costs of publication of this article were defrayed in part by the payment of page charges. Therefore, and solely to indicate this fact, this article is hereby marked “advertisement” in accordance with 18 USC section 1734. This work was supported by grants 81172083, 81371592, 81401467, 81501519, and 81571705 from the National Natural Science Foundation of China; grants 7132040, 7154188, and 7162041 from the Beijing Natural Science Foundation; and the “215 backbone program” from Beijing Municipal Commission of Health and Family Planning. No

other potential conflict of interest relevant to this article was reported.

REFERENCES

- Gould EA, Winship T, Pholbin PH, et al. Observations on a “sentinel node” in cancer of the parotid. *Cancer*. 1960;13:77–78.
- Cabanas RM. An approach for the treatment of penile carcinoma. *Cancer*. 1977;39:456–466.
- Hoogendam JP, Veldhuis WB, Hobbelenk MG, et al. ^{99m}Tc SPECT/CT versus planar lymphoscintigraphy for preoperative sentinel lymph node detection in cervical cancer: a systematic review and metaanalysis. *J Nucl Med*. 2015;56:675–680.
- Ahmed M, Purushotham AD, Horgan K, et al. Meta-analysis of superficial versus deep injection of radioactive tracer and blue dye for lymphatic mapping and detection of sentinel lymph nodes in breast cancer. *Br J Surg*. 2015;102:169–181.
- Krag DN, Weaver DL, Alex JC, et al. Surgical resection and radiolocalization of the sentinel lymph node in breast cancer using a gamma probe. *Surg Oncol*. 1993;2:335–339.
- Liang MI, Carson WE, 3rd. Biphasic anaphylactic reaction to blue dye during sentinel lymph node biopsy. *World J Surg Oncol*. 2008;6:79.
- Newman LA. Lymphatic mapping and sentinel lymph node biopsy in breast cancer patients: a comprehensive review of variations in performance and technique. *J Am Coll Surg*. 2004;199:804–816.
- Chen SL, Iddings DM, Scheri RP, et al. Lymphatic mapping and sentinel node analysis: current concepts and applications. *CA Cancer J Clin*. 2006;56:292–309.
- Alazraki NP, Eshima D, Eshima LA, et al. Lymphoscintigraphy, the sentinel node concept, and the intraoperative gamma probe in melanoma, breast cancer, and other potential cancers. *Semin Nucl Med*. 1997;27:55–67.
- Goyal A, Newcombe RG, Chhabra A, Mansel RE, ALMANAC Trialists Group. Factors affecting failed localisation and false-negative rates of sentinel node biopsy in breast cancer—results of the ALMANAC validation phase. *Breast Cancer Res Treat*. 2006;99:203–208.
- Veronesi U, Paganelli G, Viale G, et al. Sentinel lymph node biopsy and axillary dissection in breast cancer: results in a large series. *J Natl Cancer Inst*. 1999;91:368–373.
- Valdés-Olmos RA, Jansen L, Hoefnagel CA, et al. Evaluation of mammary lymphoscintigraphy by single intratumoral injection for sentinel node identification. *J Nucl Med*. 2000;41:1500–1506.
- Leidenius MH, Leppanen EA, Krogerus LA, et al. The impact of radiopharmaceutical particle size on the visualization and identification of sentinel nodes in breast cancer. *Nucl Med Commun*. 2004;25:233–238.
- Wallace AM, Han LK, Povoski SP, et al. Comparative evaluation of [^{99m}Tc] tilmanocept for sentinel lymph node mapping in breast cancer patients: results of two phase 3 trials. *Ann Surg Oncol*. 2013;20:2590–2599.
- Sondak VK, King DW, Zager JS, et al. Combined analysis of phase III trials evaluating ^{99m}Tc tilmanocept and vital blue dye for identification of sentinel

- lymph nodes in clinically node-negative cutaneous melanoma. *Ann Surg Oncol*. 2013;20:680–688.
16. Valdés Olmos RA, Tanis PJ, Hoefnagel CA, et al. Improved sentinel node visualization in breast cancer by optimizing the colloid particle concentration and tracer dosage. *Nucl Med Commun*. 2001;22:579–586.
 17. Maloney DG, Grillo-López AJ, White CA, et al. IDEC-C2B8 (Rituximab) anti-CD20 monoclonal antibody therapy in patients with relapsed low-grade non-Hodgkin's lymphoma. *Blood*. 1997;90:2188–2195.
 18. Scott SD. Rituximab: a new therapeutic monoclonal antibody for non-Hodgkin's lymphoma. *Cancer Pract*. 1998;6:195–197.
 19. Mariani G, Moresco L, Viale G, et al. Radioguided sentinel lymph node biopsy in breast cancer surgery. *J Nucl Med*. 2001;42:1198–1215.
 20. Cong L, Takeda M, Hamanaka Y, et al. Uniform silica coated fluorescent nanoparticles: synthetic method, improved light stability and application to visualize lymph network tracer. *PLoS One*. 2010;5:e13167.
 21. Malviya G, Vries E, Dierckx RA, et al. Synthesis and evaluation of ^{99m}Tc-labelled monoclonal antibody 1D09C3 for molecular imaging of major histocompatibility complex class II protein expression. *Mol Imaging Biol*. 2011;13:930–939.
 22. Wang XJ, Yang Z, Lin BH, et al. The preparation and localization study of a novel sentinel lymphoscintigraphy agent ^{99m}Tc-IT-rituximab. *Chin J Nucl Med*. 2006;26:226–230.
 23. Cousins A, Thompson SK, Wedding AB, et al. Clinical relevance of novel imaging technologies for sentinel lymph node identification and staging. *Bio-technol Adv*. 2014;32:269–279.
 24. East JM, Valentine CS, Kanchev E, et al. Sentinel lymph node biopsy for breast cancer using methylene blue dye manifests a short learning curve among experienced surgeons: a prospective tabular cumulative sum (CUSUM) analysis. *BMC Surg*. 2009;9:2.
 25. McMasters KM, Wong SL, Chao C, et al. Defining the optimal surgeon experience for breast cancer sentinel lymph node biopsy: a model for implementation of new surgical techniques. *Ann Surg*. 2001;234:292–299.
 26. Krag DN, Anderson SJ, Julian TB, et al. Technical outcomes of sentinel-lymph-node resection and conventional axillary-lymph-node dissection in patients with clinically node-negative breast cancer: results from the NSABP B-32 randomised phase III trial. *Lancet Oncol*. 2007;8:881–888.
 27. Noguchi M, Motomura K, Imoto S, et al. A multicenter validation study of sentinel lymph node biopsy by the Japanese breast cancer society. *Breast Cancer Res Treat*. 2000;63:31–40.
 28. Martin RC, Edwards MJ, Wong SL, et al. Practical guidelines for optimal gamma probe detection of sentinel lymph nodes in breast cancer: results of a multi-institutional study. for the university of Louisville breast cancer study group. *Surgery*. 2000;128:139–144.
 29. Chagpar AB, Carlson DJ, Laidley AL, et al. Factors influencing the number of sentinel lymph nodes identified. *Am J Surg*. 2007;194:860–864.
 30. Liu LC, Lang JE, Jenkins T, et al. Is it necessary to harvest additional lymph nodes after resection of the most radioactive sentinel lymph node in breast cancer? *J Am Coll Surg*. 2008;207:853–858.
 31. Estourgie SH, Nieweg OE, Olmos RA, et al. Lymphatic drainage patterns from the breast. *Ann Surg*. 2004;239:232–237.
 32. Uren RF, Howman-Giles R, Thompson J, et al. Mammary lymphoscintigraphy in breast cancer. *J Nucl Med*. 1995;36:1775–1780.
 33. Uren RF, Howman-Giles R, Renwick SB, et al. Lymphatic mapping of the breast: locating the sentinel lymph nodes. *World J Surg*. 2001;25:789–793.
 34. van Der Ent FW, Kengen RA, Van Der Pol HA, et al. Halsted revisited: internal mammary sentinel lymph node biopsy in breast cancer. *Ann Surg*. 2001;234:79–84.
 35. Tanis PJ, Nieweg OE, Valdés Olmos RA, et al. Impact of nonaxillary sentinel node biopsy on staging and treatment of breast cancer patients. *Br J Cancer*. 2002;87:705–710.
 36. Joerger M. Prevention and handling of acute allergic and infusion reactions in oncology. *Ann Oncol*. 2012;23(suppl 10):x313–x319.